

Investigation of Initial Formation of Aluminum Nitride Films by Single Precursor Organometallic Chemical Vapor Deposition of $[\text{Me}_2\text{Al}(\mu\text{-NHR})]_2$ ($\text{R} = \text{}^i\text{Pr}, \text{}^t\text{Bu}$)

Myung Mo Sung, Hyun Dam Jung[†], June-Key Lee[†], Sehun Kim^{†*},
Joon T. Park^{†*}, and Yunsoo Kim^{*}

Inorganic Materials Division, Korea Research Institute of Chemical Technology, Taejeon 305-606

[†]*Department of Chemistry, Korea Advanced Institute of Science and Technology, Taejeon 305-701*

Received September 13, 1993

The organometallic chemical vapor deposition of single precursors, $[\text{Me}_2\text{Al}(\mu\text{-NHR})]_2$ ($\text{R} = \text{}^i\text{Pr}, \text{}^t\text{Bu}$), for aluminum nitride thin films has been investigated to evaluate their properties as potential precursors. In chemical vapor deposition processes the gas phase products scattered from a Ni(100) substrate were analyzed by mass spectrometry and the deposited films were characterized by X-ray photoelectron spectroscopy (XPS). The optimum temperatures for the formation of AlN films have been found to be between 700 K and 800 K. Carbon contamination of the films seems to be attributed mainly to the methyl groups bonded to the aluminum atoms. It is apparent that $\text{}^t\text{Bu}$ group is better than $\text{}^i\text{Pr}$ group as a substituent on the nitrogen atom of the single precursors for the AlN thin film formation.

Introduction

Aluminum nitride (AlN) has received much attention due to its current and potential applications as electronic substrates, passivation and dielectric layers, high frequency surface acoustic wave devices, and optical devices.¹ Several techniques have been employed for the preparation of AlN thin films, including conventional organometallic chemical vapor deposition (OMCVD),² molecular beam epitaxy (MBE),³ and single precursor OMCVD.⁴⁻⁶ The single precursor OMCVD has been shown to have a number of important advantages over the conventional CVD process. The conventional CVD process uses, especially in the case of preparing compound films, sources that are often very corrosive, toxic and/or pyrophoric thereby necessitating extensive safety measures. In comparison, the single precursor OMCVD process uses compounds that are relatively nontoxic and not pyrophoric. With conventional multiple sources, it is not easy to obtain accurate stoichiometry. The use of single precursors makes it easy to control the stoichiometry by designing the molecules appropriate for particular deposition composition. Finally, the low temperatures (150 °C - 600 °C) often involved in single precursor OMCVD can reduce interdiffusion of layers and dopants.⁷⁻¹⁰

Cowley *et al.*¹¹ reported on the preparation of epitaxial GaAs thin film using the single precursor, $[\text{Me}_2\text{Ga}(\mu\text{-As}^t\text{Bu}_2)]_2$. We have employed the structurally similar dimeric amidolane precursors, bis(dimethyl- μ -isopropylamido-aluminum) (BDPA)¹² and bis(dimethyl- μ -*t*-butylamido-aluminum) (BDDBA)¹³ (Figure 1, *trans* forms) to prepare AlN films. Since the structures of the ligands in these precursors may play an important role in the deposition behavior, film compositions, and reaction mechanisms, it is important to find what kinds of substituents bonded to nitrogen and/or aluminum would be good for the preparation of high quality films. In this study, we investigated two AlN single precursors with R groups of $\text{}^i\text{Pr}$ and $\text{}^t\text{Bu}$ on the nitrogen atoms. To isolate the intrinsic surface reactions of these precursors from other experimen-

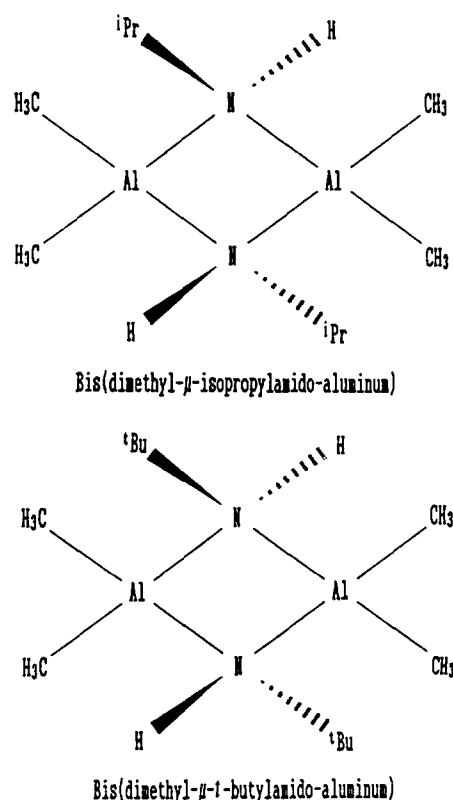


Figure 1. Molecular structures of the precursors used for the preparation of AlN films.

tal properties such as gas-phase reactions, a pressure-controlled effusive molecular beam of each of the precursors was directed onto a Ni(100) single crystal surface in an ultrahigh vacuum chamber.¹⁴ Gas phase species scattered and thermally desorbed from the crystal surface were detected by a quadrupole mass analyzer (QMA). XPS was used to analyze the deposited films.

Experimental

Synthesis of the precursors. The precursors BDPA and BDBA were prepared by the procedures reported previously.^{12,13}

Thermal Decomposition Studies. The deposition experiments were carried out in an ion-pumped UHV chamber ($P < 10^{-10}$ Torr) of the ESCALAB MK II (VG Scientific Ltd). equipped with XPS, QMA, UPS (ultraviolet photoelectron spectroscopy), a duoplasmatron ion gun, a heating-cooling sample holder, and a doser. The doser is a 3.2 mm-diameter stainless steel tube pumped by a turbomolecular pump. The dosing rate of the precursors was regulated by a variable leak valve. The precursors and the dosing line were maintained at room temperature during precursor dosing. The head gas from precursors was continuously pumped in order to minimize the contamination by the decomposed molecules in the effluent.

A Ni(100) single crystal (elliptical shape of about 0.5 cm² in area and 2 mm thick) was used as the substrate. The reason we chose Ni(100) substrate was to have a good control of temperature variation when employing resistive heating.¹⁵ The nickel crystal could be heated resistively up to 1400 K, and cooled down to 120 K using liquid nitrogen. An Alumel-Chromel thermocouple (0.25 mm in diameter) spot welded onto the side of the crystal was used to monitor the nickel crystal temperature. The nickel crystal was cleaned by repeated cycles of argon-ion sputtering (3 kV, 1 μ A/cm²) and annealing (600 K-1200 K). After each cleaning, the cleanliness of the crystal surface was confirmed by XPS and UPS.

Upon setting the crystal temperature at various values between 300 K and 970 K, 900 L of AlN precursors were sent to the nickel substrate using the doser under steady state flow condition. The deposited films on the nickel substrate were characterized by XPS. The X-ray source was Al $K\alpha_{1,2}$ (1486.6 eV), and the power was maintained at 300 W (15 kV, 20 mA). In taking photoelectron spectra, the spherical sector analyzer was operated in the constant analyzer energy mode with 20 eV pass energy, 0.1 eV step size, and 100 ms dwell time. Data acquisition and analysis were carried out by a PDP-11 Micro/R SX computer from Digital Equipment Corporation. The spectra of N 1s, Al 2p, and C 1s were synthesized using the method of least squares. Ni 2p_{3/2} peak was chosen for the substrate signal.

In the mass analysis experiments, the effusive beam of the precursors was directed onto the nickel surface from a 5 mm distance at an angle of 30° from the surface normal, and was scattered into the mass analyzer located 2 cm above the crystal and a little off-axis from the line-of-sight direction. The dosing rate of the precursors, according to the method of Henn *et al.*¹⁶ was 3.92×10^{15} molecules/s. The temperature of the nickel substrate was linearly ramped at 2 K/s.

Results and Discussion

X-ray Photoelectron Spectroscopy. After each dose of the precursors onto the clean Ni(100) surface at 300 K-970 K, the deposited films were analyzed by XPS. Figure 2a shows the atomic concentrations of the films deposited at various temperatures using BDPA. The results were re-

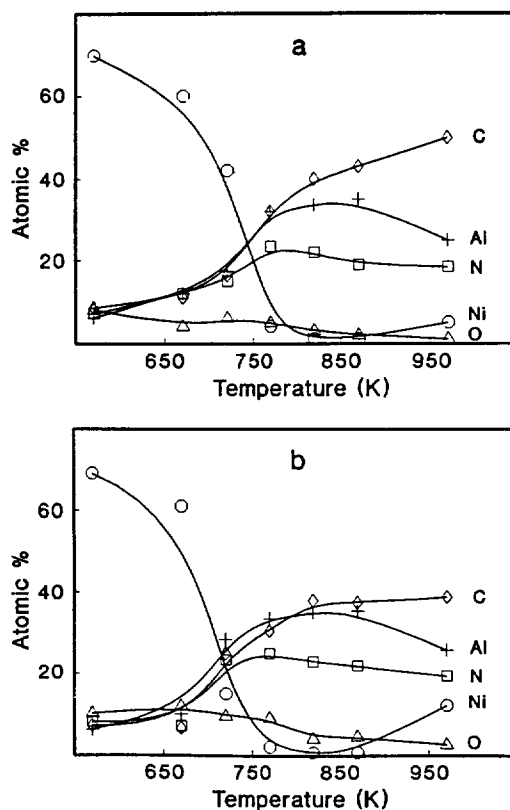


Figure 2. The atomic concentrations of the films deposited by single precursors at various temperatures (a: using BDPA, b: using BDBA).

producible through several runs. The atomic concentrations were calculated from the peak areas of the elements concerned. The substrate signal was included in the calculation as if it comes from the films, but this does not affect the general trends of the deposition behavior. At about 770 K, the nickel, aluminum, and carbon concentrations increase noticeably and the nickel signal decreases below 20%, which indicates a large increase of the deposition rate at this temperature. The deposited films contained relatively large amounts of aluminum and carbon compared to nitrogen, and the concentration of carbon is found to increase with temperature. The slight increase in the nickel signal above 900 K is probably because the deposition area at this high temperature is smaller than the viewing area of XPS. Figure 2b shows the temperature profile of the films deposited using BDBA. The deposition rate increases at around 720 K which is about 50 K lower than when BDPA was used. The films deposited from BDBA contain a little more nitrogen and less carbon than those obtained from BDPA above 720 K. The amount of carbon retained in the film does not increase noticeably above 830 K. In both cases of BDPA and BDBA, there appear signals of oxygen that were not observed on the substrate surface initially. It turns out that the precursors are rather air and moisture sensitive and form even aluminum oxide films if the vacuum condition is poor. Residual amount of oxygen containing species in the gas phase of the vacuum chamber is thought to be responsible for the appearance of the oxygen signals. The O 1s signals, however, decrease gradually in intensity with temperature.

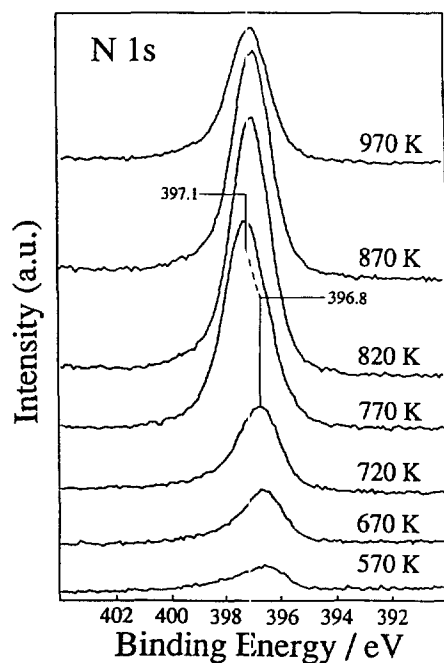


Figure 3. N 1s photoelectron spectra of the film deposited from BDPA at various temperatures.

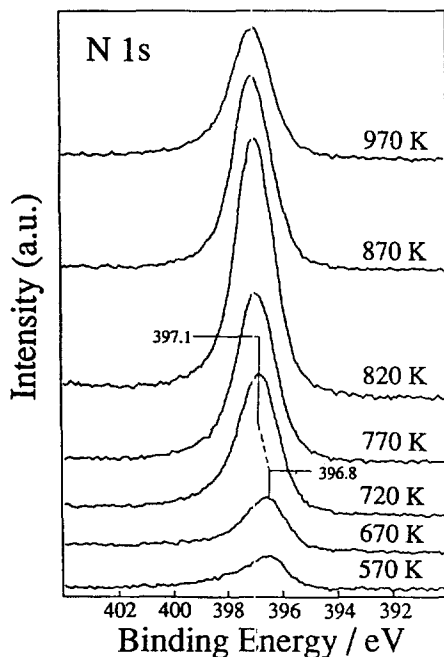


Figure 4. N 1s photoelectron spectra of the film deposited from BDPA at various temperatures.

Figure 3 and Figure 4 show the changes in the N 1s spectra of the films deposited from BDPA and BDPA, respectively, at various deposition temperatures. In Figure 3, the N 1s peak initially shows up at 396.8 eV due to the commencement of BDPA deposition, and the peak shifts 0.3 eV to the left and its half-width is narrowed at 770 K, where the deposition rate increases appreciably. The peak with the lower binding energy is probably due to the nitrogen interacting with the nickel substrate, which forms in the initial stage

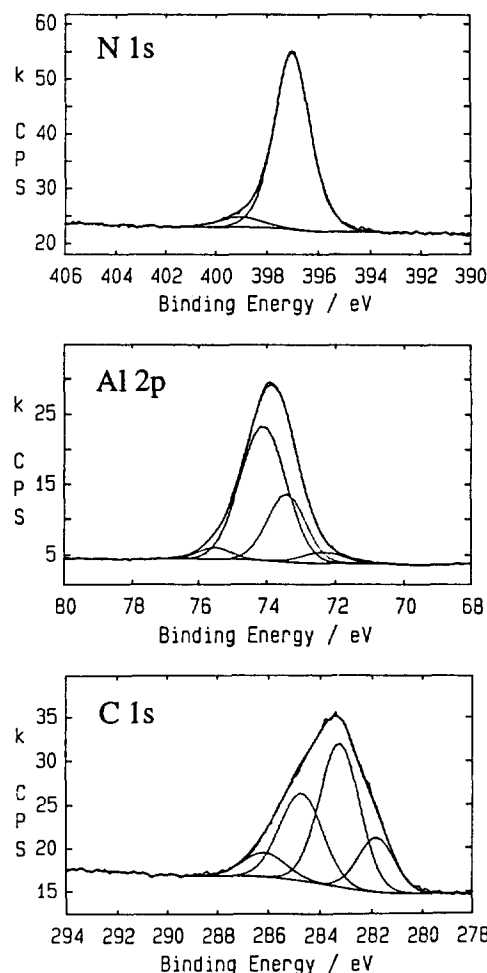


Figure 5. Curve-fitted N 1s, Al 2p, and C 1s photoelectron spectra of the film deposited from BDPA at 770 K.

of deposition. The shift of the N 1s peak from 396.8 eV to 397.1 eV is thought to be due to the deposition of a true aluminum nitride layer. Therefore the effective deposition temperature of BDPA is around 770 K. In the case of BDPA (Figure 4), the N 1s peak shifts from 396.8 eV to 397.1 eV with its half-width narrowing, and the increase in peak intensity occurs at about 720 K which is again 50 K lower than with BDPA.

Figure 5 shows synthesized N 1s, Al 2p, and C 1s spectra of the film deposited at 770 K using BDPA. In the N 1s region, the main peak appears at 397.1 eV due to AlN¹⁷ with a small peak at 398.8 eV indicating the presence of amines.¹⁸ The Al 2p region is separated into two prominent peaks with two minor peaks. The one with higher binding energy (74.2 eV) is due to AlN¹⁷ and the one with lower binding energy (73.4 eV) seems to come from methyl aluminum¹⁹ and aluminum carbide.²⁰ These two types of carbon have been known to have almost identical binding energies and so are not separable in the spectrum.²⁰ The two minor peaks at 75.6 eV and 72.3 eV are presumably due to the formation of aluminum oxide and metallic aluminum,²⁰ respectively. There are four peaks in the C 1s region corresponding to carbon associated with oxygen (286.5 eV),²⁰ the bulk carbon (284.5 eV),¹⁸ methyl carbon bonded to aluminum (283.4 eV),¹⁹ and

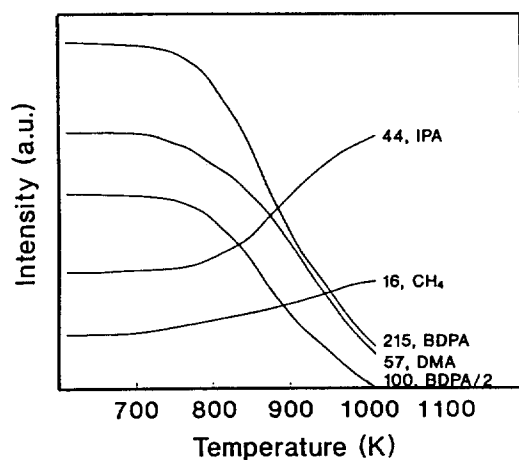


Figure 6. Temperature profiles of the scattered species when BDPA is dosed onto the nickel single crystal.

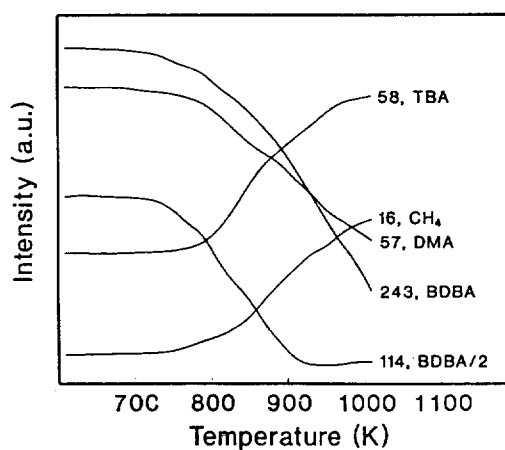


Figure 7. Temperature profiles of the scattered species when BDBA is dosed onto the nickel single crystal.

aluminum carbide (281.7 eV).²⁰ Since the peak at 283.4 eV has the highest intensity, we believe that the excess carbon mainly results from the methyl groups that were originally bonded to the aluminum atoms. The synthesized N 1s, Al 2p, and C 1s spectra of the films deposited from BDBA at 720 K show quite similar features to those of BDPA at 770 K. Bent *et al.*¹⁴ reported that surface methyl groups were responsible for the carbon incorporation at temperatures higher than 600 K in the study of thermal decomposition of triisobutylaluminum to deposit aluminum film. Recent studies of adsorption and subsequent thermal decomposition of alkyl halides have shown that CH_x ($x=1-3$) species are identified and stable on the nickel surface.²¹ Our XPS analysis is also consistent with these results in that methyl groups on aluminum atoms may subsequently decompose at higher temperatures and remain on the substrate as CH_x species, which results in higher carbon contamination in the films.

Mass analysis. In this mass analysis experiment, parent precursors in the gas phase, species scattered and thermally desorbed from the nickel substrate, and their cracking fragments all appeared in the mass spectra. The analysis of all the species in the mass spectra was too complicated to handle, so we concentrated on the peaks that showed appreciable changes in the intensities when scattering was performed. Figure 6 is the temperature profile of the intensities of the species derived from scattered BDPA, thermally decomposed fragments, and mass cracking fragments (in the residual gas analyzer) while BDPA is being directed onto the Ni(100) surface. The nickel temperature was ramped linearly at 2 K/s. In a separate experiment we observed that the parent molecular ions of BDPA and BDBA do not have the highest intensities upon fragmentation in the gas phase. Instead, the species formed by loss of a methyl group from the parent molecules dominate the fragmentation patterns. Therefore we chose $m/e=215$ (M^+-CH_3) peak for the confirmation of the presence of the parent molecule BDPA in all the mass fragmentation analysis. Similarly we chose $m/e=243$ (M^+-CH_3) peak for the analysis of BDBA. Because a simple β -cleavage of the carbon-carbon bond adjacent to nitrogen provides the most intense ion in the spectra of alkylamines,²² we chose $m/e=44$ ($\text{CH}_3-\text{CH}=\text{NH}_2^+$) for isopro-

pylamine (IPA) and $m/e=58$ ($(\text{CH}_3)_2\text{C}=\text{NH}_2^+$) for *tert*-butylamine (TBA). In Figure 6, the intensity of BDPA decreases and that of IPA increases above around 770 K which is the effective deposition temperature of BDPA. Since the intensities of dimethylaluminum (DMA, $m/e=57$) and the monomeric species (BDPA/2, $m/e=100$) decrease in the similar fashion to that of the parent molecule, these species may mainly come from the fragmentation of the parent molecules in the mass analyzer and not appreciably from thermal decomposition from the nickel surface. Methane can be formed via intramolecular reaction between methyl group and isopropyl ligand or hydrogen on nitrogen atom, and via intermolecular reaction between methyl radicals and hydrogen atoms on the surface.²³ The intensity of CH_4 ($m/e=16$) slowly increases with temperature. Because IPA is easily removed from the nickel surface but DMA isn't according to its low intensity in the mass analysis, it is thought that the deposited film has excess aluminum compared to nitrogen. The slow evolution of CH_4 implies that methyl aluminum species on the surface remain and subsequently decompose at higher temperatures, and explains why the film has large carbon incorporation.

Figure 7 shows the intensities of the species derived from BDBA with increasing temperature. Here the temperature at which the intensity of the precursor BDBA starts to decrease shows up somewhat lower (a few tens of Kelvin) than in the case of BDPA in Figure 6, which is consistent with the previous result in Figure 2. The noticeable differences in the mass spectrometric analysis of BDBA from BDPA are the slower decrease of DMA intensity, the faster increase of CH_4 intensity, and the faster decrease of the monomeric species (BDBA/2, $m/e=114$). More subtle is the behavior of the amine fragment, *tert*-butylamine (TBA), which shows highest intensity in the gas phase mass spectrum at $m/e=58$. The intensity of TBA remains almost constant beyond 720 K (up to around 780 K) which is the effective deposition temperature for BDBA. However, it is not the case with IPA which is the amine fragment from BDPA, and its intensity begins to increase around the effective deposition temperature (770 K) of BDPA as shown in Figure 6.

TBA can contribute to the intensity of DMA by losing

a hydrogen,²² but it does not seem to account for the whole intensity profile of DMA. It is not quite possible for us to speculate on the detailed surface chemistry based on the relative intensity variations of individual CH₄, DMA, and BDBA/2 species, but it is thought that their combined effects might result in the somewhat higher nitrogen content in the film by BDBA than that formed by using BDPA. The fast increase in the intensity of CH₄ (m/e=16) above 800 K explains why there is no further increase of the carbon retained in the films that are deposited above this temperature (Figure 2b).

In this investigation, qualitative comparisons were made between two kinds of precursors having different R groups on the nitrogen atoms to understand the effects of R groups on the film formation with these precursors. For both precursors, the carbon retained in the deposited films seems to come mainly from the methyl groups bonded to aluminum atoms. The change of ⁱPr group to ^tBu group is found to have three apparent beneficial effects on the deposition of the films. First, the effective deposition temperature for BDBA is 50 K lower than that for BDPA. Second, the film deposited using BDBA has less carbon incorporation compared to BDPA above 800 K. Third, ^tBu group seems to be a better substituent to retain the Al-N bonding in the CVD process than ⁱPr group, resulting in generally higher nitrogen content in the film deposited from BDBA than from BDPA.

Acknowledgments. The authors wish to express their gratitude to the Ministry of Science and Technology and Korea Science and Engineering Foundation for the financial support of this work.

References

1. Sheppard, L. M. *Ceramic Bulletin* **1990**, *69*, 1801.
2. Duffy, M. T.; Wang, C. C.; O'Clock, Jr., G. D.; McFarlane, S. H.; Zanzucchi, P. J. *J. Electron. Mater.* **1973**, *2*, 359.
3. Yoshida, S.; Misawa, S.; Itoh, A. *Appl. Phys. Lett.* **1975**, *26*, 461.
4. Interrante, L. V.; Lee, W.; McConnell, M.; Lewis, N.; Hall, E. J. *Electrochem. Soc.* **1989**, *136*, 472.
5. Ho, K.-L.; Jensen, K. F.; Hwang, J.-W.; Gladfelter, W. L.; Evans, J. F. *J. Crystal Growth* **1991**, *107*, 376.
6. Park, J. T.; Lee, J.-K.; Kim, S.; Sung, M. M.; Kim, Y. *Bull. Korean Chem. Soc.* **1993**, *14*, 163.
7. Girolami, G. S.; Jensen, J. A.; Pollina, D. M.; Williams, W. S.; Kaloyeros, A. E.; Allocca, C. M. *J. Am. Chem. Soc.* **1987**, *109*, 1579.
8. Jensen, J. A.; Gozum, J. E.; Pollina, D. M.; Girolami, G. S. *J. Am. Chem. Soc.* **1988**, *110*, 1643.
9. Gozum, J. E.; Pollina, D. M.; Jensen, J. A.; Girolami, G. S. *J. Am. Chem. Soc.* **1988**, *110*, 2688.
10. Shin, H. K.; Chi, K. M.; Hampden-Smith, M. J.; Kodas, T. T.; Farr, J. D.; Paffett, M. *Adv. Mater.* **1991**, *3*, 246.
11. Cowley, A. H.; Jones, R. A. *Angew. Chem. Int. Ed. Engl.* **1989**, *28*, 1208.
12. Amirhalili, S.; Hitchcock, P. B.; Jenkins, A. D.; Nyathi, J. Z.; Smith, J. D. *J. Chem. Soc., Dalton Trans.* **1981**, 377.
13. Al-Wassil, A.-A. I.; Hitchcock, P. B.; Sarisaban, S.; Smith, J. D.; Wilson, C. L. *J. Chem. Soc., Dalton Trans.* **1985**, 1929.
14. Bent, B. E.; Nuzzo, R. G.; Dubois, L. H. *J. Am. Chem. Soc.* **1989**, *111*, 1634.
15. Films formed on the Ni substrate invariably have more aluminum than nitrogen. The catalytic nature of nickel seems to be responsible for this result. Nevertheless, for prolonged deposition, aluminum nitride films are formed since the catalytic nature of the substrate can no longer influence the deposition. In a parallel experiment [ref. 6] we used a Si(100) substrate, and obtained almost stoichiometric ratio of aluminum and nitrogen.
16. Henn, F. C.; Bussell, M. E.; Campbell, C. T. *J. Vac. Sci. Technol. A* **1991**, *3*, 10.
17. Taylor, J. A.; Rabalais, J. W. *J. Chem. Phys.* **1981**, *75*, 1735.
18. Wagner, C. D.; Riggs, W. M.; Davis, L. E.; Moulder, J. F. *Handbook of X-ray Photoelectron Spectroscopy*; Perkin-Elmer Corporation, Physical Electronics Division, Eden Prairie: 1979.
19. Akhter, S.; Zhou, X. T.; White, J. M. *Appl. Surface Sci.* **1989**, *12*, 201.
20. Maruyama, B.; Ohuchi, F. S.; Rabenberg, L. J. *Mater. Sci. Lett.* **1990**, *9*, 864.
21. Tjandra, S.; Zaera, F. *Langmuir* **1992**, *8*, 2090, and references therein.
22. Gohlke, R. S.; McLafferty, F. W. *Anal. Chem.* **1962**, *34*, 1281.
23. Miller, J. E.; Mardones, M. A.; Nail, J. W.; Cowley, A. H.; Jones, R. A.; Eckerdt, J. G. *Chem. Mater.* **1992**, *4*, 447.